CHAPTER 146

Sediment-Cloud Based Model of Suspension over Ripple Bed due to Wave Action

Hitoshi Gotoh¹, Tetsuro Tsujimoto² and Hiroji Nakagawa³

ABSTRACT

Sediment cloud, which is released periodically from the crest of ripples, plays a very important role in suspension over a ripple bed under the wave action. By considering the special role of the sediment cloud, suspension is divided into two subprocesses: (i) the transition process from bed-load motion to suspension as the entrainment of the sediment cloud; and (ii) the diffusion process of suspended sediment released from the sediment cloud. The trajectory of the sediment cloud is calculated by Lagrangian approach in the flow field solved by $k \in model of turbulence$. The suspended sediment cloud is simulated by solving a diffusion equation which has the source term due to sediment cloud.

INTRODUCTION

Since an important role of sediment cloud on the suspension over a ripple bed was recognized from the experiment with the aid of the visualization technique (Sunamura, Bando and Horikawa (1978); Sawamoto and Yamaguchi (1979)), the model of the suspension using the characteristics of the sediment cloud began to be investigated. Sunamura (1980) proposed a formula of the sediment discharge by defining the net sediment discharge as the amount of the sediment transported more than 1.5 times of a ripple's wave length in the offshore direction. Hayakawa, Tani and Wakui (1985) applied a Lagrangian model to the suspension due to wave action over a ripple bed, by assuming the scale of sediment cloud after the experiment and solving the flow field by the Stokes's second order approximation. Swamoto and Yamaguchi

¹Research Associate, Department of Civil Engineering, Kyoto University, Yoshida Honmachi, Sakyo-ku, Kyoto, 606, Japan

²Associate Professor, Department of Civil Engineering, Kanazawa University, 2-40-20, Kodatsuno, Kanazawa, 920, Japan

³Professor, Division of Environmental Engineering, Kyoto University, Yoshida Honmachi, Sakyo-ku, Kyoto, 606, Japan

(1979) divided the flow field into two layers: (i) the "vortex layer" in which the transport by sediment cloud is predominant; and (ii) the "diffusion layer" in which the diffusion by turbulence is predominant. They estimated the one-cycle averaged turbulent intensity and the one-cycle averaged concentration of suspended sediment, based on their two layer model.

The applicability of a k- ε model of turbulence to the oscillating flow over a ripple bed was confirmed by comparing the prediction by the model to the body of the experimental data. Sato, Uehara and Watanabe (1986) performed the numerical simulation of oscillating boundary layer on the basis of the k- ε model with the equation of vorticity. They also simulated the trajectory of a suspended particle by a Lagrangian approach. Tsujimoto, Hayakawa, Ichiyama and Fukushima (1991) calculated the suspended sediment concentration by coupling the k- ε model with the diffusion equation of suspended sediment.

Sediment suspension in the oscillating flow is characterized by two factors: (i) the complexity of flow field; and (ii) the response of a suspended particle to the change of the flow field. The factor (ii) is divided into two processes: (a) the transition process form bed-load motion to suspension as the entrainment of the sediment cloud, and (b) the diffusion process of suspended sediment released from the sediment cloud. Although this hierarchical structure of sediment behavior makes the transport process more complicated, Sawamoto & Yamaguchi's model of two layer, "vortex layer & diffusion layer," which is the one-cycle averaged model, gives a good suggestion to explain this complexity. In this study, Sawamoto & Yamaguchi's model is developed to the unsteady condition, by regarding the sediment cloud as a moving source of diffusion.

The structure of the model is schematically shown in Fig. 1. The transition process by the motion of sediment cloud (subprocess (a)) is simulated by tracing the trajectory of sediment cloud in the flow field solved by a k- ε model; while the diffusion process of suspended sediment released from the sediment cloud (subprocess (b)) is simulated on the basis of the Murphy's diffusion equation (1984) with the sediment source term which expresses the generation of the sediment due to the sediment cloud.

The former is treated by the Lagrangian model which can estimate the detailed motion of the suspension; while the latter by the Eulerian model more conveniently than Lagrangian one. This model can be regarded as a fusion of the Eulerian model and the Lagrangian one by considering their advantages.

EXPERIMENT

The experiment was conducted in U-tube type oscillating

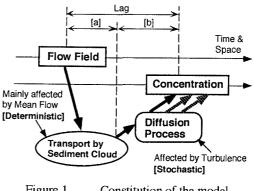


Figure 1 Constitution of the model

water tunnel with a movable bed illustrated in Fig.2. The equipment was made of acrylic resin, and the working section was 180cm long, 20cm high and 20cm wide. The access to the working section was provided by the hatches located above the central part of the water tunnel. The driving mechanism is installed to maintain the oscillation. The pump system was connected with the water tunnel at the both ends of the horizontal section, to generate the uni-directional flow. The motion of the sediment cloud was recorded by a CCD video camera from the side of the working section. The time series of the concentration of sediment near the bottom was measured by an optical turbidity meter. The test particle was a natural sand with the specific gravity 2.65 and the diameter 0.26mm. Experimental condition is shown in Table 1.

In an oscillation-current coexisting flow, the asymmetry of the flow field and that of the sediment transport due to the existence of the current bring the asymmetric ripple profile: the upstream-side slope is steeper than the downstream-side slope. The geometrical parameters of the ripple in the experimental condition is included in the range of the body of the experimental data in the wave-current coexisting flow by Watanabe, Sakinada and Isobe (1989).

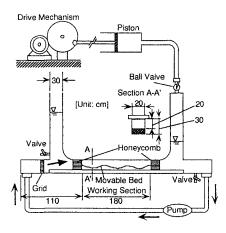


Figure 2 Oscillating water tunnel

 Table 1
 Experimental condition

Period of oscillation T (s)	2.6	
Amplitude of the mean velocity Uw (cm/s)	19.0	
Current velocity uc (cm/s)	6.2	
Ripple wavelength Lr (cm)	12.0	
Ripple waveheight Hr (cm)	2.1	
Ripple steepness Hr /Lr	0.175	
Ripple symmetry	asymmetric	
Propagating velocity of the ripple (cm/s)	-1.67	

GOVERNING EQUATIONS OVER RIPPLE BED

Orthogonal curvilinear coordinate over ripple bed:

Sawamoto (1978) proposed the orthogonal curvilinear system for the symmetric ripples. Tanaka and Syuto (1984) modified the Sawamato's system to express the asymmetric profile of ripples. The relation between the Cartesian coordinate (*x*, *y*) and the orthogonal curvilinear coordinate system (ξ , η), based on Tanaka & Syuto's method, is introduced to make a conformal mapping over the ripple bed as follows:

$$x = \xi - H_{r} \sum_{j=1}^{N} a_{r_{j}} \exp(-k_{r} j \eta) \sin(k_{r} j \xi + \theta_{r_{j}})$$

$$y = \eta + H_{r} \sum_{j=1}^{N} a_{r_{j}} \exp(-k_{r} j \eta) \cos(k_{r} j \xi + \theta_{r_{j}})$$
(1)

where H_r =ripple wave height; k_r =ripple wave number (= $2\pi/L_r$); and L_r =ripple wave length. The empirical parameter a_{rj} , θ_{rj} are determined by trial and error. The agreement between the measured ripple profile and Eq. 9 is fairly good as shown in Fig. 3.

Governing equations:

The governing equations in the orthogonal curvilinear coordinate (ξ, η) is given as follows:

$$h_{1}h_{2}\frac{\partial\phi}{\partial t} + \frac{\partial}{\partial\xi}\left(h_{2}U_{\mathrm{OR}}\phi - \Gamma_{\phi}\frac{h_{2}}{h_{1}}\frac{\partial\phi}{\partial\xi}\right) + \frac{\partial}{\partial\eta}\left(h_{1}V_{\mathrm{OR}}\phi - \Gamma_{\phi}\frac{h_{1}}{h_{2}}\frac{\partial\phi}{\partial\eta}\right) = h_{1}h_{2}S_{\phi(\xi,\eta)}$$
(2)

$$h_{1} \equiv \sqrt{\left(\frac{\partial x}{\partial \xi}\right)^{2} + \left(\frac{\partial y}{\partial \xi}\right)^{2}} ; \quad h_{2} \equiv \sqrt{\left(\frac{\partial x}{\partial \eta}\right)^{2} + \left(\frac{\partial y}{\partial \eta}\right)^{2}}$$
(3)

where ϕ =variable; Γ_{ϕ} =coefficients of apparent viscosity; and S_{ϕ} =source terms, and they are summarized in Table 2. The parameters and variables in Table 2 are as follows: $U_{\text{OR}}, V_{\text{OR}}$ = mean velocity components in ξ, η directions, respectively; P=mean pressure; ρ =mass density of fluid; Γ =effective viscosity; ν =kinematic viscos-

ity; v_t = kinematic eddy viscosity; G=production of turbulent energy; w_0 =terminal fall velocity of sediment particle; S_{cl} =source term due to the sediment cloud; and Γ_{sx} , Γ_{sy} = the coefficient of diffusion in the streamwise and vertical direction. The empirical constants are set at the recommended values by Launder and Spalding (1974) as follows: C_{μ} =0.09, $C_{1\epsilon}$ =1.44, $C_{2\epsilon}$ =1.92, σ_{k} =1.0 and σ_{ϵ} =1.3.

Although the governing equations are standard ones which are frequently used for the unsteady flow simulation, the present simulation is characterized by the sediment source term S_{cl} and its estimation mentioned later in detail. In some previous simulations, the buoyancy term, which represents the effect of suspended sediment on the flow field, is introduced into the equations of flow field. In this study, the concentration is set at the suffi-

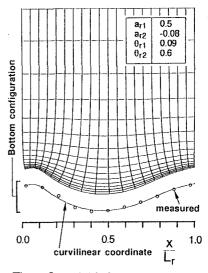


Figure 3 Grids for the calculation

φ	Γ_{ϕ}	S _{\$}	
$U_{ m OR}$		$S_{\rm U} = -\frac{1}{h_1} \frac{\partial}{\partial \xi} \left(\frac{P}{\rho}\right) + \frac{1}{h_1^2} \frac{\partial v_{\rm t}}{\partial \xi} \frac{\partial U_{\rm OR}}{\partial \xi} + \frac{V_{\rm OR}}{h_1^2 h_2} \frac{\partial v_{\rm t}}{\partial \xi} \frac{\partial h_1}{\partial \eta}$	
		$+\frac{1}{h_{1}h_{2}}\frac{\partial v_{i}}{\partial \eta}\frac{\partial V_{OR}}{\partial \xi}-\frac{U_{OR}}{h_{1}h_{2}^{2}}\frac{\partial v_{i}}{\partial \xi}\frac{\partial h_{1}}{\partial \eta}$	
V _{OR}	$v + v_t$	$S_{v} = -\frac{1}{h_{2}}\frac{\partial}{\partial\eta}\left(\frac{P}{\rho}\right) + \frac{1}{h_{1}h_{2}}\frac{\partial v_{t}}{\partial\xi}\frac{\partial U_{\text{OR}}}{\partial\eta} - \frac{V_{\text{OR}}}{h_{1}^{2}h_{2}}\frac{\partial v_{t}}{\partial\xi}\frac{\partial h_{2}}{\partial\xi}$	
		$+ \frac{1}{h_2^2} \frac{\partial v_{\iota}}{\partial \eta} \frac{\partial V_{\text{OR}}}{\partial \eta} - \frac{U_{\text{OR}}}{h_1 h_2^2} \frac{\partial v_{\iota}}{\partial \eta} \frac{\partial h_2}{\partial \xi}$	
k	$v + \frac{v_t}{\sigma_k}$	$S_{\mathbf{k}} = G - \varepsilon$	
ε	$v + \frac{v_t}{\sigma_t}$	$S_{\epsilon} = \frac{\varepsilon}{k} (C_{1\epsilon} G - C_{2\epsilon} \varepsilon)$	
С	$\frac{\Gamma_s}{S_c}$	$S_{co} = \frac{1}{h_2} \frac{\partial}{\partial \eta} (w_0 C) + S_{cl}$	
$G = v_{t} \left[2 \left\{ \left(\frac{1}{h_{1}} \frac{\partial U_{\text{OR}}}{\partial \xi} + \frac{V_{\text{OR}}}{h_{1}h_{2}} \frac{\partial h_{1}}{\partial \eta} \right)^{2} + \left(\frac{1}{h_{2}} \frac{\partial V_{\text{OR}}}{\partial \eta} + \frac{U_{\text{OR}}}{h_{1}h_{2}} \frac{\partial h_{2}}{\partial \xi} \right)^{2} \right\}$			
	$+\left(\frac{1}{h_2}\frac{\partial U_{\text{OR}}}{\partial \eta}-\frac{V_{\text{OR}}}{h_1h_2}\frac{\partial h_2}{\partial \xi}+\frac{1}{h_1}\frac{\partial V_{\text{OR}}}{\partial \xi}-\frac{U_{\text{OR}}}{h_1h_2}\frac{\partial h_1}{\partial \eta}\right)\right]$		

Table 2 Terms in governing equations

ciently low level at which the effect of the suspended sediment on the flow field is negligibly small, or the clear water flow assumption can be applied. By substituting Eq. 1 into Eq. 3, $h_1=h_2(=h_{\rm fq})$.

Boundary conditions and procedure of simulation:

The wall function is applied at the bottom boundary, or the logarithmic law of the mean velocity at the lowest point of the grid. The turbulent energy and its dissipation rate at the lowest grid point are calculated based on the local equilibrium assumption.

At the top boundary, an axial symmetric condition is applied for U, k and ε . The periodic boundary condition is applied for U, k and ε between the both side boundaries. The present simulation does not require the boundary condition of concentration at the bottom, which is usually employed in the calculation of the concentration, because the sediment source term is added in the present simulation. Therefore, the concentration profile can be evaluated by the present simulation without giving the sediment concent

tration at the reference level.

The governing equations are discretized by SIMPLE algorithm by Patankar and Spalding (1972), and the calculation was conducted based on TEACH code (Gosman and Ideriah (1976)). For the conversion assessment of the flow field, the following conditions are subjected: (i) the summation of the absolute residual in each cell of a continuity equation is less than 1% of the flow discharge in the streamwise direction; (ii) the absolute residual in each cell of a mean flow equation is less than 1% of the total momentum at the inflow boundary.

The procedure of the present simulation are as follows: (i) to solve the flow field ; (ii) to simulate the motion of the sediment cloud by Lagrangian method in the flow field solved in the process (i); (iii) to evaluate the sediment source term in the equation of concentration based on the trajectories of the sediment cloud determined in the process (ii); and (iv) to solve the equation of concentration in the flow field determined in the process (i) with the sediment source term evaluated in the process (iii).

SOLUTION OF FLOW FIELD

The characteristics of the calculated flow field are discussed at the phase $2\pi/5$ and $7\pi/5$. The change of the bulk mean velocity at the inflow boundary is given in the cosine pattern, hence the velocity in the current direction is maximum at the phase 2π , and the velocity against the current direction is maximum at the phase π .

The calculated mean velocity field at the phase $2\pi/5$ and $7\pi/5$ are shown in Fig. 4. The vortex due to the separation is found in the lee side of ripples at the phase $2\pi/5$; while the vortex is not clearly simulated at the phase $7\pi/5$. The asymmetric ripple profile affects strongly on the flow field.

Figure 5 shows the calculated distribution of the turbulent energy. At the phase $2\pi/5$, the high value area is recognized along the outer edge of the vortex due to the separation; while at the phase $7\pi/5$, the high energy area due to the vortex is not found. The non-uniformity of the turbulent energy in the streamwise direction at the phase

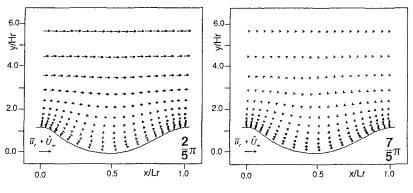
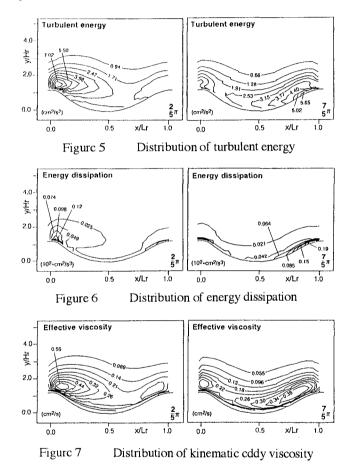


Figure 4 Mean velocity vector

 $2\pi/5$ is smaller than that at the phase $7\pi/5$, hence the contour lines at the phase $7\pi/5$ become more parallel to the bottom profile than those at the phase $2\pi/5$. Fig. 6 shows the calculated energy dissipation, and Fig. 7 shows the calculated kinematic eddy viscosity. Their asymmetric distributions due to the asymmetric bottom profile are found in both figures. The calculated results suggest the drastic change of the kinematic eddy viscosity, which are usually used to estimate the coefficient of the diffusion of suspended sediment.



SIMULATION OF SEDIMENT CLOUD MOTION

Simulation model:

The sediment cloud was defined only qualitatively in the previous studies as the mixture of sediment and fluid which is apparently like a cloud; while the quantitative

definition of the sediment cloud is not clear because the boundary between the sediment-fluid mixture and the surrounding fluid is ambiguous. In order to clarify the qualitative definition of the sediment cloud, it is here idealized as follows: a "kernel" exists at the central part of the cloud in which the all of the sediment transported by the cloud is contained. The kernel is not affected by the turbulence, hence the trajectory of the kernel is a deterministic one ruled by the mean velocity filed.

Here, the kernel is approximated by the rigid cylinder. By neglecting a rotating motion of the cylinder, the equation of the motion of the kernel is written as follows:

$$\rho\left(\frac{\sigma_{\rm cl}}{\rho} + C_{\rm M}\right) A_2 d_{\rm cl}^2 \frac{\mathrm{d}\mathbf{u}_{\rm cl}}{\mathrm{d}t} = -\frac{1}{2} C_{\rm D} \rho A_1 d_{\rm cl} |\mathbf{u}_{\rm cl} - \mathbf{u}_{\rm f}| (\mathbf{u}_{\rm cl} - \mathbf{u}_{\rm f}) + \rho(1 + C_{\rm M}) A_2 d_{\rm cl}^2 \frac{\mathrm{d}\mathbf{u}_{\rm f}}{\mathrm{d}t} - \rho\left(\frac{\sigma_{\rm cl}}{\rho} - 1\right) \mathbf{g} A_2 d_{\rm cl}^2$$

$$(4)$$

where \mathbf{u}_{cl} =velocity vector of the kernel; \mathbf{u}_{f} =velocity vector of the surrounding fluid; \mathbf{g} =gravitational acceleration; d_{cl} =diameter of the kernel; C_{M} =added mass coefficient; σ_{cl} =density of the kernel; and A_{1} , A_{2} =one- and two dimensional geometrical coefficients. The drag coefficients C_{D} is given by

$$C_{\rm D} = C_{\rm Deo} + \frac{24}{R_{\rm e}} \quad ; \quad R_{\rm e} = \frac{d_{\rm el} |\mathbf{u}_{\rm el} - \mathbf{u}_{\rm f}|}{\nu} \tag{5}$$

Although the coefficient $C_{D\infty}$ depends on the shape of the particle, $C_{D\infty}$ sets 0.4 in this study. It is smaller than that of cylinder, because the real kernel is not a rigid body.

Equation 4 is applicable to the orthogonal curvilinear coordinate (ξ, η) only with the modification of the gravity term as follows:

$$\begin{bmatrix} g_{\xi} \\ g_{\eta} \end{bmatrix} = \frac{1}{h_{fq}^2} \begin{bmatrix} \frac{\partial y}{\partial \eta} & -\frac{\partial x}{\partial \eta} \\ -\frac{\partial y}{\partial \xi} & \frac{\partial x}{\partial \xi} \end{bmatrix} \begin{bmatrix} 0 \\ g \end{bmatrix} = \begin{bmatrix} -\frac{1}{h_{fq}^2} \frac{\partial x}{\partial \eta} g \\ \frac{1}{h_{fq}^2} \frac{\partial x}{\partial \xi} g \end{bmatrix}$$
(6)

Following the definition of the kernel mentioned above, the velocity of the surrounding fluid in Eq. 4 is given by the mean velocity of the flow field. By considering that the sediment cloud is generated by the vortex due to the separation, the diameter of the kernel d_{cl} is related to the scale of the vortex, or the ripple wave height as follows:

$$d_{\rm cl} = \beta_{\rm dcl} H_{\rm r} \quad ; \quad \beta_{\rm dcl} = 0.1 \tag{7}$$

Here, the kernel is treated by the deterministic equations, hence the probabilistic aspect of the suspension, namely the random motion of the suspended sediment should not be included in the kernel. In general, the number of the random suspended sediment increases with the distance from the center of the sediment cloud. Hence, the kernel with small diameter is adopted in this study.

The mass density of the kernel σ_{cl} is given in a following form.

$$\sigma_{\rm cl} = \sigma \frac{q_{\rm scl}}{q_{\rm cl}} + \rho \left(1 - \frac{q_{\rm scl}}{q_{\rm cl}} \right) \tag{8}$$

where q_{cl} =volume of the sediment cloud; and σ =density of sand. The volume of the contained sediment q_{scl} is estimated in a following manner. The volume of the sediment released from the sediment cloud (kernel) per unit time is assumed to be proportional to the volume of the contained sediment. Hence, the volume of contained sediment in the kernel is given by following equation.

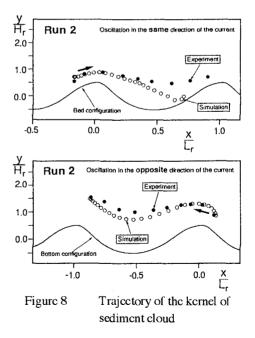
$$\frac{q_{\rm scl}}{q_{\rm scl0}} = \exp\left(-\frac{\zeta_{\rm cl}}{\beta_{\rm cl}T_{\rm D}}\right) \quad ; \quad \zeta_{\rm cl} = t - t_{\rm cl0} \tag{9}$$

where q_{scl0} =initial volume of the contained sediment; T_D =life time of the sediment cloud; β_{cl} =the empirical constant; and t_{cl0} =starting time of the sediment cloud, or the time at which the main stream changes their direction. An observation of the motion of sediment clouds in the experiment suggested that the life time of the sediment cloud approximately coincides the period of the oscillation; and that the diffusion is active in the half period of oscillation from t_{cl0} to the time when the central position of the cloud is difficult to determine. By considering these results of the observation, T_D and β_{cl}

are set $T_D=T$, (=period of oscillation); and $\beta_{cl}=0.2$. By setting $\beta_{cl}=0.2$, the volume of the contained sediment after a half period from t_{cl0} is about 10% of the initial volume of the contained sediment.

Trajectory of the sediment cloud:

Figure 8 shows the simulated trajectory of the kernel with the experimental data. In the simulation, the initial position of the kernel is determined by the experiment. The experimental data were obtained as a following manner: (i) the motion of the sediment cloud was recorded by a CCD video camera from the side wall of the water tunnel; (ii) the position of the center of the sediment cloud, which was defined as the position with the highest concentration of sediment by a visual judgment, in



each 1/10 seconds was determined; (iii) the deterministic trajectory was determined by averaging the trajectories given in the process (ii).

When the oscillation occurs in the opposite direction of the current, the agreement between the simulation and the experiment is fairly good. While, under the oscillation in the same direction of the current, the result of the simulation deviates form the experimental result after the cloud passes the trough of the ripple. The concentration of the sediment decreases with the increase of the travelling time of the cloud, hence the reliability of the experimental results, which depends on the concentration, decreases with the increase of the travelling time of the cloud. Furthermore, the volume of the contained sediment decreases with the increase of the travelling time of cloud, therefore the role of the kernel as a source of the sediment in the diffusion equation becomes less important with the travelling time of cloud. Hence the deviation of trajectory never bring a severe error in the simulation explained in the following chapter.

SIMULATION OF SUSPENSION

Estimation of the source term:

The sediment source term found in Murphy's diffusion equation are estimated as follows:

$$S_{\rm cl}(\xi,\eta,t) = -\chi_{\rm cl}(\xi,\eta,t) \frac{\mathrm{d}q_{\rm scl}}{\mathrm{d}t}$$
(10)

Where $\chi_{cl}(\xi,\eta,t)$ =the distribution of the suspended sediment around the center of the sediment cloud, and the uniform distribution is here supposed. Then, $\chi_{cl}(\xi,\eta,t)$ is written as follows:

$$\chi_{\rm el}(\xi,\eta,t) = \begin{cases} 1 & \text{when} & (\xi,\eta) = (\xi_{\rm el},\eta_{\rm el}) \\ 0 & \text{other} \end{cases}$$
(11)

where (ξ_{cl}, η_{cl}) =the location of the center of the sediment cloud.

Estimation of the diffusion coefficient:

Although the diffusion coefficient of suspended sediment is usually estimated by assuming it's similarity to the kinematic eddy viscosity, the motion of the suspended sediment is affected not only by the fluid motion, the characteristics of the variation of which is represented by the kinematic eddy viscosity; but also by the response of the particle to the change of the surrounding fluid motion. Tsujimoto and Nakagawa (1986) proposed the estimation of the diffusion coefficient on the basis of the similarity between the diffusion equation and the continuous expression of the random walk model. In this section, the diffusion coefficient is estimated based on the Tujimoto and Nakagawa's method.

By considering the equilibrium state of the random walk of suspended sediment in the vertically one-dimensional infinite space, the following relation is obtained.

2022

$$\frac{\mathrm{E}[\zeta^2]}{2}\frac{\partial f_{\mathrm{s}}}{\partial y} = \mathrm{E}[\zeta] \cdot f_{\mathrm{s}}$$
(12)

where, f_s =probability density of existing height of suspended sediment, and ζ =vertical deviation of suspended sediment during Δt . Δt =time step of random walk. On the other hand, the one-dimensional diffusion equation in a steady state which is written as follows:

$$\varepsilon_{\rm s} \frac{dC_{\rm s}}{dy} = -w_0 \cdot C_{\rm s} \quad ; \quad C_{\rm s} = C_{\rm m} \cdot f_{\rm s} \tag{13}$$

where C_m =depth-averaged concentration of suspended sediment. By comparing Eqs. 12 and 13 to each other, and supposing the relation $E[\zeta]=w_0\Delta t$, the diffusion coefficient can be written as follows:

$$\varepsilon_{\rm s} = \frac{\mathrm{E}[\zeta^2]}{2\Delta t} = \frac{\mathrm{E}[\zeta]^2 + \sigma_{\zeta}^2}{2\Delta t} = \frac{w_0^2 \Delta t}{2} + \frac{\sigma_{\zeta}^2}{2\Delta t} \tag{14}$$

The magnitude of the deviation of the suspended sediment during Δt , σ_{ζ} , is given in a following form, by introducing one-dimensional Markovian process to express the characteristics of the turbulence.

$$\sigma_{\zeta}^{2} = 2k_{0s}^{2}\sigma_{v}^{2}\left[\Delta t \cdot T_{L} - \Delta t^{2}\left\{1 - \exp\left(-\frac{\Delta t}{T_{L}}\right)\right\}\right]$$
(15)

where σ_v =the standard deviation of the surrounding fluid velocity during Δt , and k_{0s} =the parameter of the particle's response. Finally, by substituting Eq. 15 into Eq. 14, the turbulent Schmidt number S_c is written as follows:

$$\frac{1}{S_{\rm c}} \equiv \frac{\varepsilon_{\rm s}}{v_{\rm t}} = \frac{\varepsilon_{\rm s}}{\sigma_{\rm v}^2 T_{\rm L}} = \frac{1}{2} \left(\frac{w_0}{\sigma_{\rm v}} \right)^2 \Xi_{\rm s} + k_{0\rm s}^2 \{ 1 - \Xi_{\rm s} (1 - e^{\Xi_{\rm s}}) \} \quad ; \quad \Xi_{\rm s} = \Delta t / T_{\rm L}$$
(16)

In the homogeneous turbulent flow, the Lagrangian time scale T_L can be written in the following form through a dimensional consideration as follows:

$$T_{\rm L} \cong \frac{3v_{\rm t}}{2k} \tag{17}$$

The Lagrangian time scale can be related to the parameters of the flow field by Eq. 17.

Figure 9 shows the distribution of turbulent Schmidt number estimated by Eq. 16 with the time step of the simulation $\Delta t=0.01$ s. At the phase $2\pi/5$, at which the separation occurs, the spatial non-uniformity is strong; while at the phase $7\pi/5$, the spatial non-uniformity is small, or the contour line is almost parallel to the bottom configuration. Although Eq. 16 is derived by assuming the diffusion in the one-

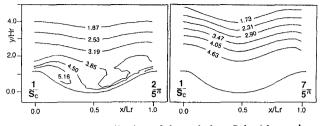


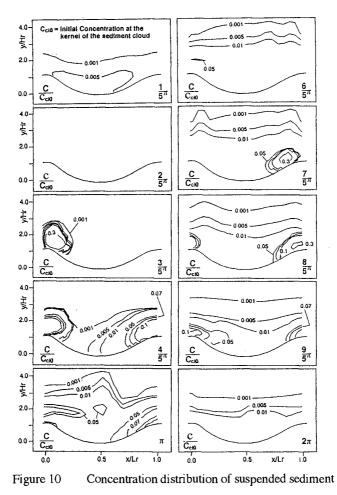
Figure 9 Distribution of the turbulent Schmidt number

dimensional uniform field $(-\infty,\infty)$, the fundamental mechanism of the motion of suspended sediment: the characteristics of the response of suspended sediment to the turbulence; and the fundamental characteristics of the turbulent flow field are included in this equation. Therefore, the estimation of the diffusion coefficient based on Eq. 16 is better than the usual way of estimation, in which a linear proportionality is assumed between kinematic eddy coefficient and the diffusion coefficient.

RESULTS OF SIMULATION AND DISCUSSION

Figure 10 shows the result of the simulation on the distribution of the concentration of suspended sediment. The value on each contour line implies the relative concentration to the initial concentration of the kernel (= C_{cl0}), and the phase shown in each figure is the phase of the balk mean flow. Although the experiment shows that many of bed-load particles are entrained into the separation zone and high density sediment is recognized in the separation zone; the present simulation never treats the sediment in the separation zone as suspended sediment, the definition of which is the sediment in a random motion. Because the motion of the sediment in a separation zone is strongly ruled by the motion of vortex, and it is rather deterministic. Therefore, the high concentration region is not found at the phase $2\pi/5$ in the simulation, in which the separation is found in the lee side of ripples.

The sediment cloud propagating in the opposite direction to the current (leftward in Fig.9), which emerges at the phase $3\pi/5$, moves in the upstream direction (leftward in Fig.9) with generating high density suspended sediment, and then it reaches the region above the steep slope of the upstream neighboring ripple (right-hand side mild sloop in Fig.9) at the phase $4\pi/5$. At the phase π , the sediment cloud exists above a trough of ripple, and it plays a role to push the contour lines up. At the phase $6\pi/5$, high concentration region due to the sediment cloud is not found clearly, and the concentration is almost uniform in the horizontal direction. While the sediment cloud propagating in the same direction to the current (rightward in Fig. 9), which emerges at the phase $7\pi/5$ above the mild slope of the ripple, reaches the region above the steep slope in the downstream neighboring ripple. At the phase $9\pi/5$, the high-concentration region extends to the downstream direction. At the phase 2π , the contour lines are almost parallel to each other, and the concentration profile is approximately uniform in the horizontal direction.



From the phase 2π to $2\pi/5$, the deposition of the sediment is promoted and the contour lines move in the downward direction, because the sediment cloud, or the source of sediment, does not exist; while, from the phase $7\pi/5$ to 2π , the speed of the downward motion of the contour lines is suppressed due to the existence of the sediment cloud. Although the sediment cloud moving in the same direction of the current is smaller than that moving in the opposite direction to the current, it plays a role to maintain the high-concentration region which is generated by the motion of the sediment cloud moving in the opposite direction of the current.

Figure 11 shows the comparison between the simulated time series of the concentration and that obtained by the experiment at the two points: [A] the concentration

at the point near the crest located within the trajectory of the sediment cloud; and [B] the concentration at the point near the trough. The initial volume of the contained sediment is determined to fit the peak of the concentration of the Fig.10 [A]. Although the peak-phase of the simulation is smaller than that of experiment, the relative height of the second peak to the first peak is simulated fairly well in Fig. 10 [A]. Fig. 10 [B] shows that, at the trough, the fundamental features of the experimental results are simulated: the existence of the first peak and the gradual transition from the first to the second peak.

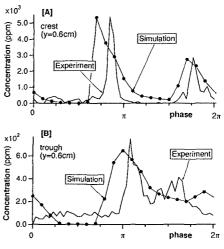


Figure 11 Time series of concentration

CONCLUSION

The results obtained in this study are summarized as follows:

(1) The oscillation-current coexisting flow over a ripple bed is numerically simulated by a k- ε model of turbulence. The result of the simulation shows that an asymmetry of the bottom-neighboring structure of the flow is induced clearly from a slight asymmetry of the ripple profile.

(2) To simulate the motion of the sediment cloud as the moving source of the suspended sediment in the field of the diffusion, the existence of a kernel is supposed at the central part of the sediment cloud. The motion of the kernel is simulated based on the equation of motion of a rigid cylinder. The result of the simulation agrees well with the experiment of the trajectory of sediment cloud.

(3) The turbulent Schmidt number is estimated on the basis of the similarity between the stochastic model of the suspension and the diffusion model. The spatial non-uniformity of the Schmidt number indicates the importance of the improvement of previous method which requires an assumption of a linear proportional relation between the kinematic eddy viscosity and the diffusion coefficient.

(4) The concentration profile is simulated by Murphy's diffusion equation with sediment source term, to connect a Langrangian approach of the motion of sediment cloud with an Eulerian approach based on the diffusion equation. From the results of the simulation, the important role of the sediment cloud on the diffusion of suspended sediment over a ripples is clarified.

ACKNOWLEDGMENT

The authors express their sincere gratitude to Messrs. Masaru Senba & Mikihiro

Watanabe (former Graduate Students, Kyoto University) for their help in the experiment.

APPENDIX-REFERENCES

- Gosman, A. D. and Ideriah, J. K. (1976). "TEACH-T, A general computer program for two-dimensional, turbulent, recirculating flows." Dept. of Mech. Eng., Imperial College of Tech., London, S. W. 7.
- Hayakawa, N., Tani, M. and Wakui, M. (1985). "Mechanism of sand transport and transport rate over sand ripples due to wave action." *Proc. 32th Japanese Conf.* on Coastal Eng., 288-292, (in Japanese).
- Launder, B. E. and Spalding, D. B. (1974). "The numerical computation of turbulent flow." *Computer method in applied mech. and Eng.*, Vol. 3.
- Murphy, P. J. (1984). "Equilibrium boundary condition for suspension", Jour. Hydraul. Eng. ASCE, Vol. 111, No. 1, 1613-1640.
- Patankar, S. V. and Spalding, D. B. (1972). "A calculation procedure for heat, mass and momentum transfer in three-dimensional parabolic flows." Int. Jour. Heat Mass Transfer, Vol. 15, 1787.
- Sato, S., Uehara, H. and Watanabe, A.(1986). "Numerical simulation of the oscillatory boundary layer flow over ripples by a k- ε turbulence model." *Coastal Eng. in Japan, JSCE*, Vol. 29, 65-78.
- Sawamoto, M. (1978). "The conformal mapping of the semi-infinite region over a wavy boundary." *Proc. JSCE*, Vol. 216, 29-35.
- Sawamoto M. and Yamaguchi S. (1979). "Theoretical modeling on wave entrainment of sand particles form rippled beds." *Proc.JSCE*, Vol. 288, 107-113, (in Japanese).
- Sunamura, T., Bando, T. and Horikawa, K. (1978). "An experimental study of sand transport mechanism and rate over asymmetrical sand ripples." *Proc. 25th Japanese Conf. on Coastal Eng.*, 250-254, (in Japanese).
- Sunamura, T. (1980). "A laboratory study on-offshore transport of sediment and a model for eroding beaches." Proc. 17th Coastal Eng. Conf., ASCE, 1051-1070.
- Tanaka, H. and Syuto, N. (1984). "Experimental study on an oscillatory flow combined with a steady motion over a wavy wall." *Proc. 31th Japanese Conf. on Coastal Eng.*, 301-305, (in Japanese).
- Tsujimoto, G., Hayakawa, N., Ichiyama, M., Fukushima, Y. and Nakamura, Y. (1991). "A study on suspended sediment concentration and sediment transport mechanism over rippled sand bed using a turbulence model." *Coastal Eng. in Japan, JSCE*, Vol. 34, No. 2, 177-189.
- Tsujimoto, T. and Nakagawa, H. (1986). "Saltation and suspension." Proc. 3rd Int. Symp. on River Sedimentation, Mississippi, USA, 777-786.
- Watanabe, A., Sakinada, M. and Isobe M. (1989). "Ripple formation and sand transport rate in a wave-current coexisting system." *Proc. Coastal Eng.*, Vol. 36, 229-303, (in Japanese).